Carbohydrate Polymers 169 (2017) 441–450

Contents lists available at ScienceDirect

Carbohydrate Polymers

journal homepage: www.elsevier.com/locate/carbpol

Antibacterial and antioxidative activity of *O*-amine functionalized chitosan

Tamer M. Tamer[a,b], Mohamed A. Hassan[c], Ahmed M. Omer[a], Katarína Valachová[b], Mohamed S. Mohy Eldin[a,d], Maurice N. Collins[e,*], Ladislav Šoltés[b]

[a] *Polymer Materials Research Department, Advanced Technologies and New Materials Research Institute (ATNMRI), City of Scientific Research and Technological Applications (SRTA-City), New Borg El-Arab City Alexandria, Egypt*
[b] *Laboratory of Bioorganic Chemistry of Drugs, Institute of Experimental Pharmacology and Toxicology, Bratislava, Slovakia*
[c] *Protein Research Department, Genetic Engineering and Biotechnology Research Institute (GEBRI), City of Scientific Research and Technological Applications (SRTA-City), New Borg El-Arab City, Egypt*
[d] *Chemistry Department, Faculty of Science, University of Jeddah, Osfan, Saudi Arabia*
[e] *Stokes Laboratories, Bernal Institute, University of Limerick, Ireland*

ARTICLE INFO

Article history:
Received 11 November 2016
Received in revised form 10 April 2017
Accepted 12 April 2017
Available online 21 April 2017

Keywords:
Chitosan derivatives
Staphylococcus aureus
Bacillus cereus
Escherichia coli
Pseudomonas aeruginosa

ABSTRACT

Cinnamaldehyde was immobilized to *O*-amine functionalized chitosan *via* a coupling reaction. Fourier transform infrared spectroscopy confirmed *N*-cinnamyl substitution. Wetting analyses demonstrate more hydrophobicity in the *N*-cinnamyl substituted *O*-amine functionalized chitosan compared to chitosan or unsubstituted *O*-amine functionalized chitosan. Thermal gravimetric analysis and differential scanning calorimetry demonstrates that the prepared *N*-cinnamyl substituted *O*-amine functionalized chitosan exhibits higher thermostability than unmodified chitosan at temperatures in which polysaccharides are commonly stored and utilised. The *N*-cinnamyl substituted *O*-amine functionalized chitosan, against four different bacteria strains [two gram-positive (*Staphylococcus aureus* and *Bacillus cereus*) and two gram-negative (*Escherichia coli* and *Pseudomonas aeruginosa*)], displays promotion of inhibition activity against these bacterial strains. Finally, the antioxidative activity of the *N*-cinnamyl substituted *O*-amine functionalized chitosan was compared with those activities of chitosan and *O*-amine functionalized chitosan. This was evaluated by uninhibited and inhibited hyaluronan degradation and ABTS assay. The *N*-cinnamyl substituted *O*-amine functionalized chitosan shows a lower activity towards donating a hydrogen radical compared to chitosan or *O*-amine functionalized chitosan. On the other hand, the *N*-cinnamyl substituted *O*-amine functionalized chitosan exhibited a higher ability to scavenge the $ABTS^{\bullet+}$ cation radical compared to chitosan and *O*-amine functionalized chitosan.

1. Introduction

Chitosan is a biodegradable, renewable polysaccharide that generally is considered to be biocompatible and non-toxic (Baldrick, 2010; Kean & Thanou, 2010). It is the second most abundant polysaccharide after cellulose; and is commonly derived from crustacean shells. Chitin consists of ß-(1→4)-2-acetamido-2-deoxy-D-glucopyranose (GlcNAc) as a repeating unit, while chitosan has been produced by deacetylation of chitin with a deacetylation degree greater than 60%. Chitosan has been employed in various applications ranging from cosmetics, artificial skin, wound healing, antimicrobial, photography, food and nutrition, ophthalmology and wastewater treatment (Albadarin, Collins, Khraisheh, Walker, & Mangwandi, 2017; Dodane and Vilivalam, 1998; El-Sayed, Tamer, Omer, & Mohy Eldin, 2016; Jeon, Shahidi, & Kim, 2000; Kenawy, Abdel-Hay, Mohy Eldin, Tamer, & Ibrahim, 2015; Kumar, Muzzarelli, Muzzarelli, Sashiwa, & Domb, 2004; Mohy Eldin, Soliman, Hashem, Tamer, & Sabet, 2013; Shahidi, Arachchi, & Jeon, 1999; Soliman, El-Kousy, Abd-Elbary, & Abouzeid, 2013). Unlike other polysaccharides, the unique properties of chitosan are attributed to free amine groups, which provide its basic character. In 2015 (Mohy Eldin, Hashem, Omer, & Tamer,

Abbreviations: ABTS, 2,2′- azinobis-[3-ethylbenzothiazoline-6-sulfonic acid] diammonium salt; DMEM, Dulbecco's modified Eagle's medium supplemented; DMSO, dimethyl sulfoxide; EDA, Ethylene diamine; GlcNAc, ß-(1→4)-2-acetamido-2-deoxy-D-glucopyranose; HA, hylauronan; LB broth, Luria-Bertani broth; MTT, 3-(4,5-dimethythiazol-2-yl)-2,5-diphenyltetrazolium bromide; pQ, para-benzoquinone; ROS, reactive oxygen species; WBOS, Weissberger biogenic oxidative system.

* Corresponding author.
E-mail address: Maurice.Collins@ul.ie (M.N. Collins).

http://dx.doi.org/10.1016/j.carbpol.2017.04.027
0144-8617/

2015a) first describe the synthesis of a cinnamyl chitosan schiff base using varying mole ratios of chitosan and cinnamaldehyde. The influence of reaction condtions on chitosan coupling were studied. These materials showed increasing antibacterial activity against both gram negative and gram positive bacteria with increasing the degree of substitution. Mohy Eldin et al. further this work to determine the physio-chemical properties of the resulting cinnamyl chitosan schiff base (Mohy Eldin, Hashem, Omer, & Tamer, 2015b). The reader is referred to Kutyrev, 1991 for a deeper understanding of the chemistries involved.

Recently, some of the current authors have produced antioxidant–chitosan conjugates by immobilization of antioxidative molecules onto chitosan chains (Tamer, Valachova, Mohy Eldin, & Soltes, 2016a; Tamer, Valachova, Mohyeldin, & Soltes, 2016b). In Tamer et al. (2016a); aromatic derivatives were prepared by coupling cinnamaldehyde group with chitosan amine groups. Results showed that an increase of cinnamaldehyde ratio leads to improvement in antimicrobial activity. However, at higher concentration, the Schiff base becomes insoluble which reduces its antimicrobial benefits.

In Tamer et al., 2016b; results show that free radical scavenging activity of chitosan was increased via the amination process. The promotion of antioxidant activity was attributed to replacing hydroxyl groups with free amine groups. Here, we combine these two approaches to produce a schiff base of O-amine chitosan with the goal of producing enhanced antibacterial and antioxidative activity. The o-amine functionalized chitosan (reported in Tamer et al., 2016b) has been used throughout this manuscript as a secondary control material with pure chitosan being the primary control.

The destructive impact of reactive oxygen species (ROS) against living cells brings about damage and ultimately leads to cell death. ROS include superoxide anion radicals, hydroxyl radicals, and hydrogen peroxide that are generated as byproducts of metabolic processes inside cells or in environmental sources. However, ROS can readily react with a broad range of essential biomolecules (Anselmo & Cobb, 2004; Baek et al., 2008; Waris & Ahsan, 2006). Antioxidants, which are scavengers of free radicals, can quench, delay or inhibit ROS formation. They protect biomolecules from damage by competing for existing radicals and removing them from the reaction (Kim & Rajapakse, 2005; Xiong, Li, Jin, & Chen, 2007). Consequently, the use of antioxidants as preventive and as therapeutic agents is of great interest to the scientific and medical community.

Here we report cinnamaldehyde addition to O-amine functionalized chitosan. Cinnamaldehyde is the main constituent of Cinnamon oil (70–90%) and has various biological activities. It demonstrates a strong and broad activity against both gram-negative and positive pathogenic bacteria. The pro-oxidant activity of Cinnamon as an essential oil has been shown to be effective in overcoming local tumor volume or tumor cell proliferation through necrotic and apoptotic effects (Stammati et al., 1999).

Chitosan and its derivates have been shown to possess marked antimicrobial activity (Badawy & Rabea, 2011; dos Santos, Dockal, & Cavalheiro, 2005; Dutta, Tripathi, & Dutta, 2011; Friedman & Juneja, 2010; Gavalyan, 2016; Kumar et al., 2014; Kong, Chen, Xing, & Park, 2010; Raafat & Sahl, 2009; Rabea, Badawy, Stevens, Smagghe, & Steurbaut, 2003; Vinsova & Vavríková, 2011). Chitosan's antimicrobial activity has been demonstrated to be associated with disruption of the prokaryotic cell membrane and its entry into the cell nucleus (Krajewska, Wydro, & Janczyk, 2011). Chitosan derivative material with novel architecture may provide opportunity to explore and modify chitosan's antimicrobial activity. Recently, there has been a growing interest in antioxidants from different sources for dietary, pharmacological and biomedical uses. Recently, there has been a growing interest in obtaining antioxidants from different sources for dietary, pharmacological and biomedical uses.

Therefore, the aim of this study was to characterize the chemical structure of the newly synthesized *N*-cinnamyl substituted *O*-amine functionalized chitosan. Thermal, antibacterial and antioxidative properties of the synthesized chitosan derivative were assessed in comparison with those properties of native and *O*-amine functionalized chitosan.

2. Materials and methods

2.1. Materials

Chitosan and *O*-amine functionalized chitosan with medium molecular weight were prepared and supplied from Advanced Technology and New Materials Research Institute (ATNMRI), New Borg El-Arab City Alexandria, Egypt. The high-molar-mass hyaluronan (HA) Lifecore P9710-2A was kindly donated by Lifecore Biomedical Inc., Chaska, MN, USA (M_w = 808.7 kDa; M_w/M_n = 1.63). The analytical purity grade NaCl and $CuCl_2{\cdot}2H_2O$ (Slavus Ltd., Slovakia); l-ascorbic acid and $K_2S_2O_8$ (p.a. purity, max 0.001% nitrogen; Merck, Germany); 2,2′-azinobis-[3-ethylbenzothiazoline-6-sulfonic acid] diammonium salt (ABTS; purum, ≥99%; Fluka, Germany) were used as received. Acetic acid, ethanol, p.a., sulfuric acid (99.9%), dimethylsulfoxide, potassium bromide (≥99.9%), LB broth, Dulbecco's modified Eagle's medium, fetal bovine serum 3-(4,5-dimethythiazol-2-yl)-2,5-diphenyltetrazolium bromide, trypsin, ethylenediamintetraacetic acid, *p*-benzoquinone, ethylenediamine, sodium hydroxide were purchased from Sigma-Aldrich, Germany. Cinnamaldehyde (98%) was supplied from Scharlau, Spain. Deionized high-purity grade H_2O, with conductivity of ≤ 0.055 μS/cm, was produced by using the TKA water purification system (Water Purification Systems GmbH, Germany).

2.2. Preparation of the N-cinnamyl substituted O-amine functionalized chitosan

Chitosan (1 g) was dissolved in 50 ml of 2% acetic acid under stirring at room temperature for 6 h. The resulting viscous solution was filtered through a cheesecloth to remove undissolved particles. This solution was stirred for 6 h at 50 °C during which hydroxyl groups were activated by *para*-benzoquinone (pQ) (see supplementary information) in order to incorporate extra amine groups through reaction with ethylene diamine (EDA) (Mohy Eldin et al., 2015a; Tamer et al., 2016a; Kutyrev, 1991). The resulting dark yellow gel (O- amine functionalised chitin) was deacetylated using 50% NaOH to produce O- amine functionalised chitosan as shown in Scheme 1. Then 10 ml of ethanol containing 0.3 g of cinnamaldehyde was added to the solution under stirring to produce *N*-cinnamyl substituted *O*-amine functionalized chitosan via SN2 mechanism. The *N*-cinnamyl substituted *O*-amine functionalized chitosan was then added to the excess of 2% ethanol sodium hydroxide solution. The precipitate was filtered and washed several times with water and ethanol to remove unreacted cinnamaldehyde. The obtained fine brown powder was filtered and dried in a vacuum oven at 60 °C overnight.

2.3. Water uptake

Water uptake (%) was measured by placing a weighed dry sample in distilled water for six hours. After reaching the equilibrium swelling, the sample was filtered off and weighed. The water uptake was calculated as follows:

$$\text{Wateruptake}(\%) = \{[M - M_0]/M_0\} \times 100$$

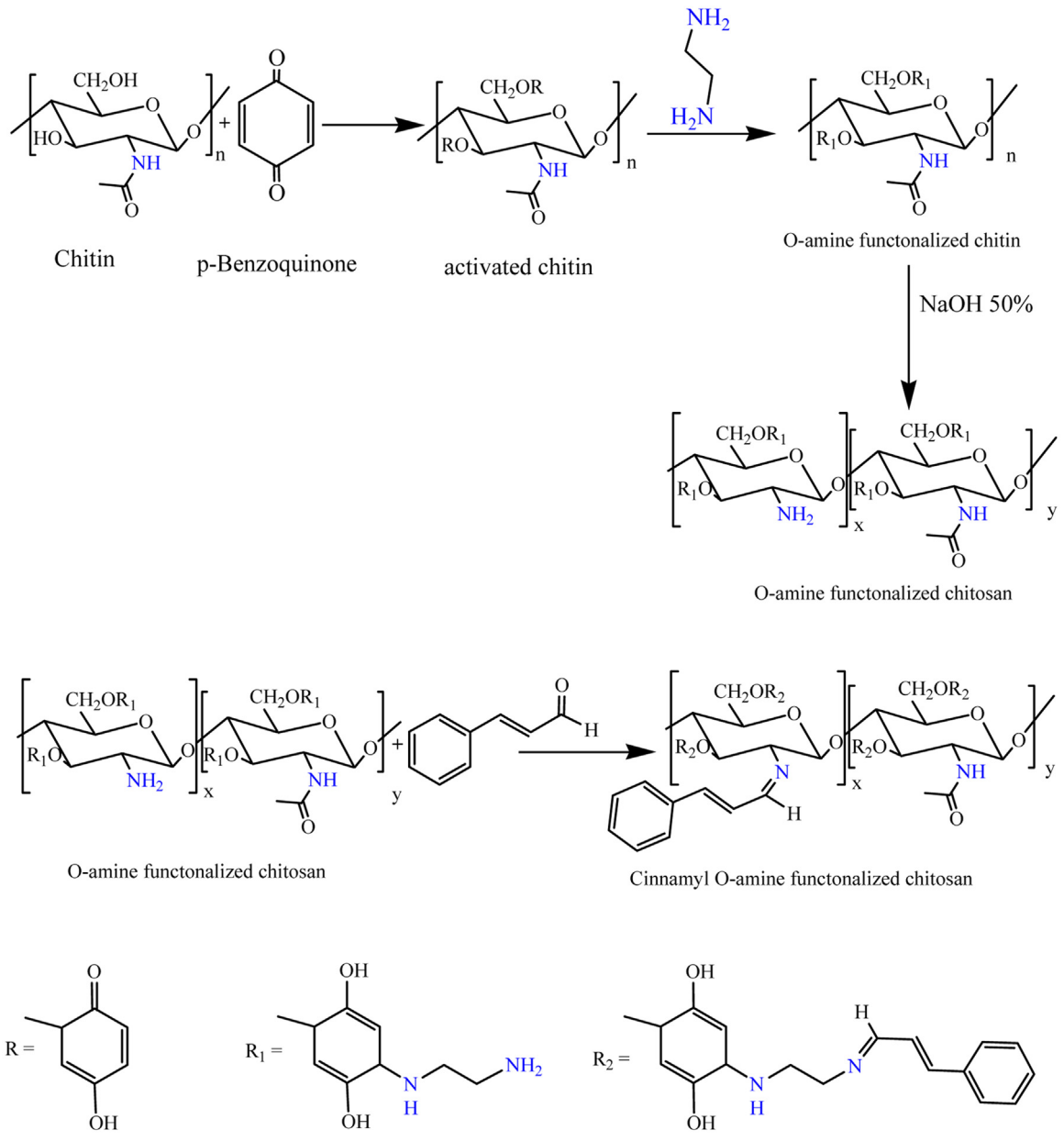

Scheme 1. Preparation of the *N*-cinnamyl substituted *O*-amine functionalized chitosan.

where **M** is the weight of the swollen sample and $\mathbf{M}_0$ is the weight of the dry sample. All measurements were in triplicate.

2.4. Moisture content

The sample weighed previously was kept in a chamber with a humidity level of 80% overnight and then weighed before and after drying in vacuum oven at 90 °C for 6 h. Water content was calculated as follows:

$$\text{Moisturecontent}(\%) = \{[\mathbf{M} - \mathbf{M}_0]/\mathbf{M}_0\} \times 100$$

where **M** is the weight of the sample before drying and $\mathbf{M}_0$ is the weight of the dry sample. All measurements were in triplicate.

2.5. Determination of ion exchange capacity

Chitosan or chitosan derivatives (0.1 g) were dissolved in 20 ml of 0.1 M H_2SO_4 on shaking for 3 h. The mixture was than filtered and an aliquot was titrated against a standard solution of sodium hydroxide. Similarly, a control titration without the addition of chitosan was also performed. The ionic capacity of chitosan samples were calculated using the following equation:

$$\text{Ionexchangecapacity} = \{(\mathbf{V}_2 - \mathbf{V}_1) \times \mathbf{a}\}/\mathbf{w}(\text{meq/g})$$

where $\mathbf{V}_2$ and $\mathbf{V}_1$ are the volumes of NaOH solutions required for complete neutralization of H_2SO_4 in the absence and presence of the polymer, respectively, and **a** is the normality of NaOH and **w** is the weight of sample taken for analysis (Mohy Eldin et al., 2015a; Ramnani & Sabharwal, 2006). All measurements were in triplicate.

2.6. Fourier transfer infrared spectroscopy (FT-IR)

Functional groups in the chemical structure of chitosan and its derivatives were identified using a FT-IR spectrophotometer (Shimadzu FTIR-8400S, Japan) and the data were analyzed using the IR Solution software, version 1.21. The polymer sample (1 – 2 mg) was

added to KBr (200 mg) and scanned between 4000 and 400 cm^{-1} using 30 scans at a resolution of 4 cm^{-1}.

2.7. Thermogravimetric analysis (TGA)

TGA analysis of chitosan and chitosan derivatives were carried out using a thermogravimetric analyzer (Shimadzu TGA-50, Japan) in temperatures ranging from 25 to 800 °C under nitrogen atmosphere at a gas flow rate of 20 ml/min and a heating rate of 10 °C/min.

2.8. Differential scanning calorimetry (DSC)

Differential scanning calorimetry of chitosan and its derivatives were carried out by using a DSC analyzer (Shimadzu DSC-60A, Japan) in temperatures ranging from 0 to 350 °C under nitrogen atmosphere at a gas flow rate of 50 ml/min and a heating rate of 10 °C/min. All thermal measurements were carried out on single samples and used for comparative purposes against control samples.

2.9. Scanning electron microscopy (SEM)

Scanning electron images of samples of chitosan and of its derivatives were captured using a scanning electron microscope (Joel Jsm 6360LA, Japan). The analyzed samples were fixed on a specimen mount with carbon paste. The surface of samples was coated with a thin layer of gold to eliminate poor conductivity of the sample's current before testing.

2.10. Broth evaluation method

Antimicrobial activity of chitosan and its derivatives were measured according to the reported method (Skyttä & Mattila, 1991). Briefly, the bacteria were incubated in Luria-Bertani medium (LB medium) (1% peptone, 0.5% yeast extract, and 1% NaCl, pH = 6). The inoculation was conducted at 37 °C for 24 h while shaking. The obtained bacterial suspension was diluted with the previous peptone medium solution. Then, 0.1 ml of diluted bacteria suspension was cultured in 10-ml liquid peptone medium, and dissolved in various amounts of the tested polymer (10, 20, 40, and 50 mg). The inoculated medium remained shaking at 37 °C for 24 h. After incubation, the optical density of each well was determined (TF). Bacterial growth inhibition of chitosan and the chitosan derivative were reported as inhibition percentage (%) by the following equation (Eq. (2)), according to Moreno-Vásquez et al. (2017):

$$\text{Inhibition}(\%) = 1 - (T_{\text{fsample}} - T_{0\text{sample}}) - (T_{\text{fblank}} - T_{0\text{blank}})/ T_{\text{fgrowth}} - T_{0\text{growth}}) - (T_{\text{blank}} - T_{0\text{blank}}) \times 100 \quad (2)$$

where $T_{0sample}$ and $T_{Fsample}$ are the optical densities at 620 nm of the strain growth in the presence of pure chitosan or modified chitosan before (T_0) and after (T_F) incubation, respectively; T_{0blank} and T_{Fblank} corresponded to the medium with pure chitosan (Pka = 6.2) or modified chitosan (Pka = 6.2) before and after incubation, respectively; and T_0 growth and T_F growth correspond to the strain growth in the presence of medium (positive control) before and after incubation, respectively. The number of bacteria was counted by using the ultraviolet absorbance of culture medium at 620 nm. Measurements were carried out in triplicate.

2.11. Cytotoxicity studies in vitro

The cell viability was carried out on NIH 3T3 (mouse fibroblast cell line) and was evaluated using MTT [3-(4,5-dimethythiazol-2-yl)-2,5-diphenyltetrazolium bromide] assay (Mosmann, 1983). The fibroblast cells were cultured in 50 cm^2 culture flask including complete Dulbecco's modified Eagle's medium (DMEM) supplemented with 10% fetal bovine serum at 37 °C, 5% CO_2 and 85% humidity. The culture was observed until it became confluent and the cells were harvested by adding 0.05% trypsin/EDTA and incubated at 37 °C, and 5% CO_2 for 5 min for detaching the cells completely. Trypsin was neutralized using DMEM medium, and the cell suspension was centrifuged at 1200 rpm for 10 min and the cells were re-suspended in DMEM. The cells were counted *via* light microscope using trypan blue and haemocytometer.

Different amount (25, 50, 100, 150, and 200 mg) of chitosan, *O*-amine functionalized chitosan and the *N*-cinnamyl substituted *O*-amine functionalized chitosan powder were applied for evaluation of their cytotoxic response. The investigated materials were sterilized by embedding in 70% ethanol, and then washed four times with sterilized PBS. The materials were dried and exposed to UV light illumination in laminar flow for 30 min under steril conditions (Hassan, Amara, Abuelhamd, & Haroun, 2010). The fibroblast cells were seeded in a 96-wells tissue culture plate at numbers 4×10^3 cells/well. The total volume of each well was 200 μl with the tested material, but the control wells contained the cells without material. The test was carried out in triple wells for each sample. The plate was incubated at 37 °C, and 5% CO_2 for 2 days. After incubation, the medium was removed from each well, and the wells were washed three times with sterilized PBS to remove the materials and cell debris. Twenty μl of MTT (5 mg/ml) was added to each well, and the plate was shaken for 5 min at 120 rpm. The plate was incubated at 37 °C for 4 h. Following the incubation period, 200 μl of dimethylsulfoxide (DMSO) was added to each well and shaken again for 5 min at 120 rpm to dissolve the formed formazan crystals. The results were recorded in triplicate, and the percentage of viable cells was calculated by comparing with control.

2.12. Evaluation of biodegradability

Degradation activities of chitosan and its derivatives were determined by colorimetric method of Miller (1959) using the dinitrosalicylic acid (DNS-reagent). This method is based on determination of color developed after reaction between reducing sugars liberated from polysaccharide and DNS-reagent. Procedure: Two ml of phosphate buffer (pH 7.0) including 100 mg of samples were transferred to 2 ml Eppendorf. Next 0.5 ml of lysozyme solution was added to it and incubated for 24 h at 37 °C. Blanks were prepared by incubated samples in the same way without enzyme. The determination was carried out in triplicate. After incubation, enzyme activity was stopped by adding 1.5 ml DNS-reagent; tubes were placed in a boiling water-bath for 15 min, cooled down to room temperature. Optical density of the samples was immediately measured at 575 nm.

2.13. ABTS method

For the ABTS decolorization assay, the $ABTS^{\bullet+}$ was pre-formed by the reaction of an aqueous solution of $K_2S_2O_8$ (3.3 mg) in H_2O (5 ml) with ABTS (17.2 mg). The resulting bluish green radical cation solution was stored overnight in the dark below 0 °C. Before performing experiments, the solution (1 ml) was diluted with acetic acid solution (0.5%) to a final volume of 60 ml. A modified ABTS assay (Rapta, Valachova, Gemeiner, & Soltes, 2009) was used to test the radical-scavenging capacity of chitosan and its derivatives using a UV-1800 spectrophotometer (SHIMADZU, Japan). The UV/VIS spectra were recorded in defined times in 1-cm quartz UV cuvette after mixing the solutions of chitosan and its derivatives (50 μl) with the $ABTS^{\bullet+}$ solution (2 ml).

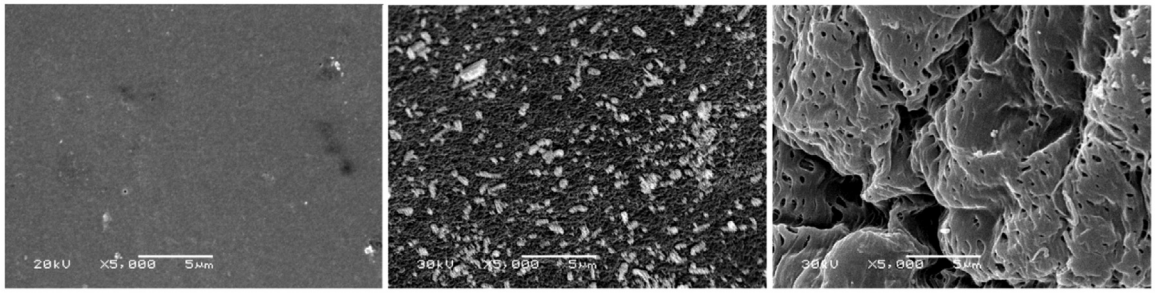

Fig. 1. SEM images of chitosan, *O*-amine functionalized chitosan and the *N*-cinnamyl substituted *O*-amine functionalized chitosan.

2.14. Uninhibited/inhibited HA degradation

A volume of 50 μl of 160 μM $CuCl_2$ solution was added to 7.9 ml of hyaluronic acid (HA) solution (2.5 mg/ml) HA solution and after stirring for 30 s the mixture was left to stand for 7 min 30 s at room temperature. For more in-depth analysis of HA solution behavior the reader is referred to (Collins and Birkinshaw, 2013a, Tamer, Valachova, & Soltes, 2014; Collins and Birkinshaw, 2013b). Then, 50 μl of ascorbic acid solution (16 mM) was added to the reaction mixture, stirred for 30 s and immediately transferred into the viscometer Teflon® cup reservoir.

The procedures to investigate the pro- and antioxidative effects of acetic acid, chitosan or its derivatives were as follows:

- A volume of 50 μl of 160 μM $CuCl_2$ solution was added to the HA solution (7.85 ml), and the mixture, after a 30-s stirring, was left to stand for 7 min 30 s at room temperature. Then, 50 μl of acetic acid (0.5%) or 50 μl of chitosan or its derivatives (4.92 mg/ml) dissolved in acetic acid (0.5%) was added and followed by stirring again for 30 s. Finally, 50 μl of ascorbic acid solution (16 mM) was added to the reaction mixture, stirred for 30 s and immediately transferred into the viscometer Teflon® cup reservoir.
- A procedure similar to that described in procedure (a) was also applied after standing for 7 min 30 s at room temperature, 50 μl of ascorbic acid solution (16 mM) was added to the reaction mixture and stirred for 30 s. And after 1 h 50 μl of acetic acid (0.5%), chitosan or its derivatives were added to the reaction mixture, followed by 30-s stirring and immediately transferred into the viscometer Teflon® cup reservoir. The changes in dynamic viscosity of the HA reaction mixture (8 ml) in viscometer Brookfield LVDV-II-PRO digital rotational viscometer (Brookfield Engineering Labs., Inc., Middleboro, MA, USA) were recorded 2 min after the onset of the experiments at 25.0 ± 0.1 °C in 3-min intervals for up to 5 h. The viscometer Teflon® spindle rotated at a constant 180 rpm, at a shear rate equaling 237.6 s^{-1} (Soltes, Stankovska, Kogan, Gemeiner, & Stern, 2005; Soltes et al., 2007).

3. Results and discussion

In order to improve antibacterial and antioxidant properties of chitosan, the *N*-cinnamyl substituted *O*-amine functionalized chitosan as a new derivative was prepared and characterized. As shown in Scheme 1, primary amine groups of *O*-amine functionalized chitosan were coupled with the aldehyde group of cinnamaldehyde to produce the corresponding Schiff base of the *N*-cinnamyl substituted *O*-amine functionalized chitosan.

3.1. Physicochemical properties of chitosan and its derivatives

It is well known that hydrophilicity of biomaterials strongly influences the interaction of materials with live cells. Water uptake values for chitosan, *O*-amine functionalized chitosan (whose properties have been previously reported in Tamer et al., 2016b) and the *N*-cinnamyl substituted *O*-amine functionalized chitosan were 171.5 ± 3.5, 231.7 ± 6.8 and 91.7 ± 5.7%, respectively. Results of water absorption demonstrate a significant increase in water uptake of O-amine functionalized chitosan derivative that was lower after coupling with cinnamaldehyde. The coupling of amine groups with cinnamaldehyde replaced hydrophilic groups with an aromatic group that subsequently reduces the polymer hydrophilicity. Results of water uptake and the moisture content in polymers indicate their hydrophilic nature: the content of moisture was 7.9 ± 1.2, 12.8 ± 2.7 and 13.8 ± 0.8% for chitosan, *O*-amine functionalized chitosan and the *N*-cinnamyl substituted *O*-amine functionalized chitosan, respectively. Increased hydrophilicity of *O*-amine functionalized chitosan was responsible for elevating its moisture content. An unexpected slight increase in the moisture content in case of the *N*-cinnamyl substituted *O*-amine functionalized chitosan is attributed to the formation of pores along the surface, which infers its pseudohydrophilic character (Mohy Eldin et al., 2015a) as shown in Fig. 1.

Fig. 1 shows the microstructure of the polymer surfaces. It is clear that there is an increase in surface roughness and pores were observed on the surface through coupling amine groups with cinnamaldehyde. The mechanism behind this is unclear, but it may be associated with distortion of chain alignment and/or solvent evaporation during processing.

3.2. Ion exchange capacity

Surface free amine groups of chitosan and its derivatives were determined by ion exchange capacity, which was 4.9, 6.2 and 4.2 meq/g for chitosan, *O*-amine functionalized chitosan and the *N*-cinnamyl substituted *O*-amine functionalized chitosan, respectively. A higher content of amino groups in *O*-amine functionalized chitosan resulted in increasing its ion exchange capacity. On the other hand, the decrease in ion exchange capacity of the *N*-cinnamyl substituted *O*-amine functionalized chitosan, in comparison to the capacity of chitosan, was attributed to consumption of surface free amine groups when coupling with cinnamaldehyde.

3.3. FT-IR

Fig. 2 illustrates the regular bands of chitosan function groups. A broad band between 3200 – 3600 cm^{-1} corresponds to the stretching vibration of NH_2 and OH groups. Bands between 2835 – 2950 cm^{-1} is a combination of C—H stretching of methyl and methylene groups, bands at 1620 cm^{-1} point out stretching vibration of C=O and NH—C=O functional groups. Bands at 1066 – 1059 cm^{-1} correspond to C—O—H group stretching. A new band at 1642 cm^{-1} was generated that is attributed to C=N vibrations characteristic of imines (Tamer et al., 2015). This band is not

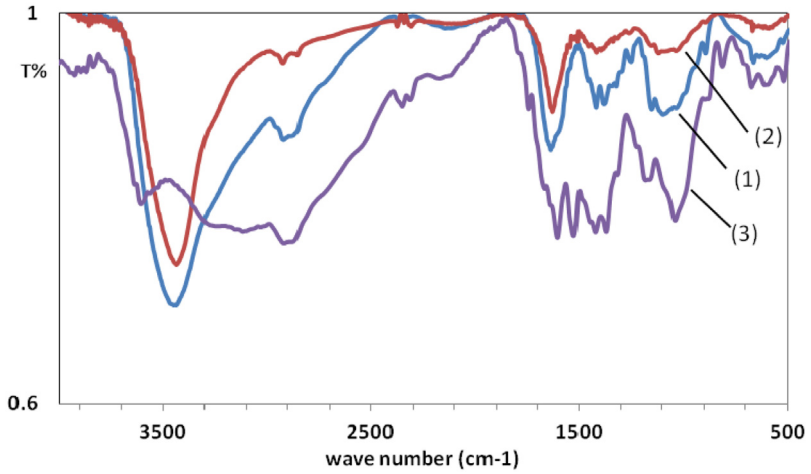

Fig. 2. FT-IR spectrum of chitosan (1), *O*-amine functionalized chitosan (2) and the *N*-cinnamyl substituted *O*-amine functionalized chitosan (3).

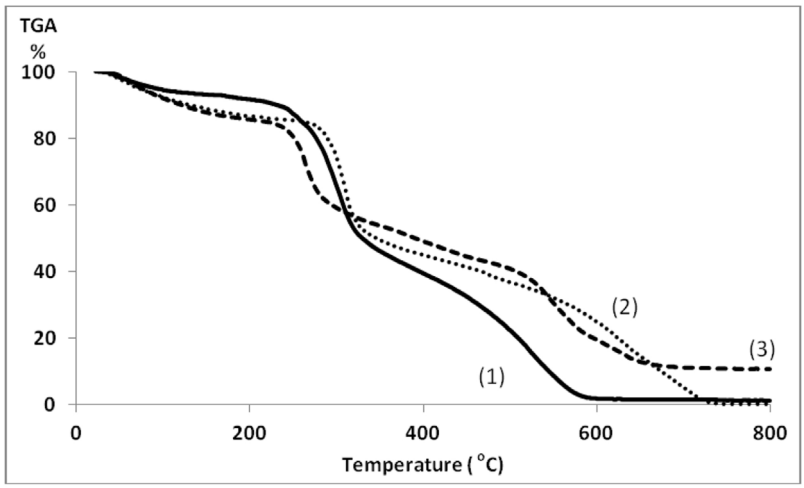

Fig. 3. Thermal gravimetric analysis of chitosan (1), *O*-amine functionalized chitosan (2) and the *N*-cinnamyl substituted *O*-amine functionalized chitosan (3).

observed in chitosan. On the other hand, there is no evidence of bands characteristic of free aromatic aldehydes near to 1665 cm^{-1}. The bands at 1580 cm^{-1} were a result of C=C stretching in the aromatic aldehyde ring.

3.4. Thermal gravimetric analysis

Fig. 3. represents thermal gravimetric analysis of chitosan, *O*-amine functionalized chitosan and the *N*-cinnamyl substituted *O*-amine functionalized chitosan.

The first decline from ambient temperature to about 200 °C can be attributed to the moisture content in the sample. The weights of chitosan, *O*-amine functionalized chitosan and the *N*-cinnamyl substituted *O*-amine functionalized chitosan were reduced by 8.4, 13.3 and 14.4% respectively. *O*-Amine functionalized chitosan rather than chitosan has an increased content of water that may be explained by higher hydrophilicity due to the increased number of free amine groups along the polymer backbone.

The subsequent degradation of all polymers was observed from 220 °C to 320 °C. Degradation of chitosan, *O*-amine functionalized chitosan and the *N*-cinnamyl substituted *O*-amine functionalized chitosan in this phase were 38.1, 29.6 and 28.2%, respectively. It was a result of oxidative decomposition of the chitosan backbone. In this stage, the first depression was due to destruction of amine groups to form crosslinked fragments. Overall, the *N*-cinnamyl substituted *O*-amine functionalized chitosan displays better thermal stability and this can possibly be attributed to thermally induced crosslinking reactions (Pawlak & Mucha, 2003; Zawadzki & Kaczmarek, 2010) which may play a role in the antibacterial and antioxidative properties.

3.5. Differential scanning calorimetry

Fig. 4 shows the clear endothermic band around 100 °C that is attributed to evaporation of moisture content of samples: an increase in moisture content was observed in the range chitosan, *O*-amine functionalized chitosan, and the *N*-cinnamyl substituted *O*-amine functionalized chitosan in accordance with previous results.

The second thermal event is an exothermic peak that corresponds to thermal decomposition of a pyranose ring (Kittur, Harish Prashanth, Udaya Sankar, & Tharanathan, 2002; Pawlak & Mucha, 2003; Sreenivasan, 1996; Zawadzki & Kaczmarek, 2010). The peaks (see Fig. 4) in chitosan and *O*-amine functionalized chitosan are seen almost in the same range (starting from 290 °C to 325 °C), where in the *N*-cinnamyl substituted *O*-amine functionalized chitosan the peaks appear between 225 °C to 280 °C. The shift of the exothermal band in the *N*-cinnamyl substituted *O*-amine functionalized chitosan to lower temperature may be attributed to a

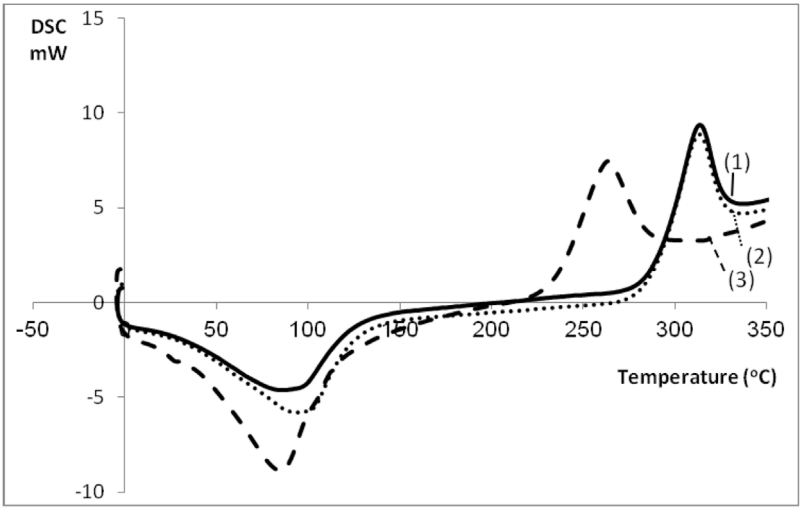

Fig. 4. Differential scanning calorimetric measurements of chitosan (1), *O*-amine functionalized chitosan (2) and the *N*-cinnamyl substituted *O*-amine functionalized chitosan (3).

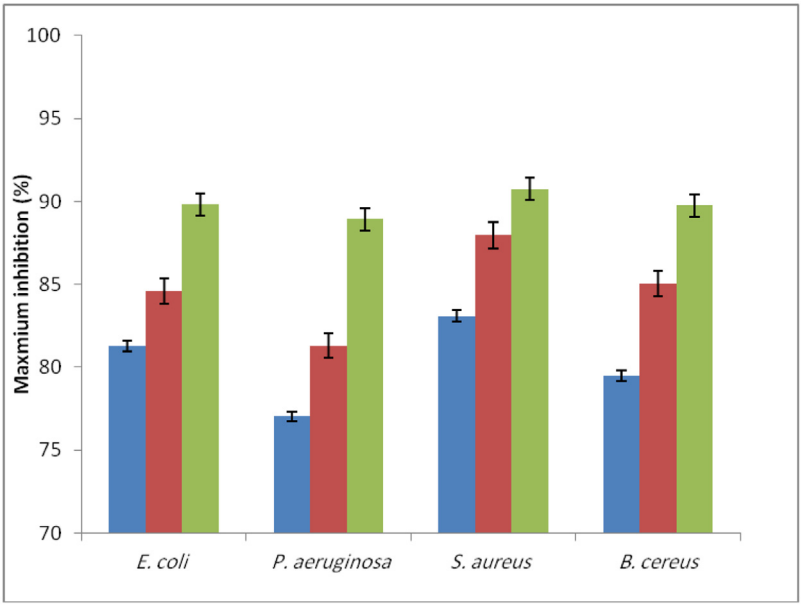

Fig. 5. Antibacterial activity of chitosan (blue), *O*-amine functionalized chitosan (red) and the *N*-cinnamyl substituted *O*-amine functionalized chitosan (green) against different bacterial strains (the polymer concentration 4 mg/ml), broth media pH = 6 and incubated at 37 °C. (For interpretation of the references to colour in this figure legend, the reader is referred to the web version of this article.)

coupling of amine groups with cinnamaldehyde that accelerated thermal decomposition of backbone pyranose ring.

3.6. Antibacterial evaluation

Fig. 5 demonstrates a general increase of antibacterial activities of the *N*-cinnamyl substituted *O*-amine functionalized chitosan against investigated bacteria compared to chitosan and *O*-amine functionalized chitosan. The antibacterial activities of the *N*-cinnamyl substituted *O*-amine functionalized chitosan against *E. coli, P. aeruginosa, S. aureus and B. cereus* were 89.8, 88.9, 90.7 and 89.7%, respectively recording the best performance of materials tested.

The *O*-amine functionalized chitosan has the greater antibacterial activities than chitosan due to the increasing number of NH_3^+ groups, which maximize the ionic interaction. (Mohy Eldin, Soliman, Hashem, & Tamer, 2008; Mohy Eldin et al. 2012). On the other hand, the *N*-cinnamyl substituted *O*-amine functionalized chitosan has less free amine groups, but the incorporation of phenolic groups improved its antibacterial activity. Since the presence of phenolic groups increases the hydrophobicity the *N*-cinnamyl substituted *O*-amine functionalized chitosan can interact with peptidoglycan of the cell wall and lipoprotein in the outer membrane specifically of gram-negative bacteria. Hence, this interaction results in a block of the channels that are responsible for exchange of electrolytes and nutrients. This chemical interaction gives the *N*-cinnamyl substituted *O*-amine functionalized chitosan significant activities against gram-negative and gram-positive bacteria. It is worth noting that the molecular weight of chitosan in this study is a medium molecular weight, thus it can penetrate the cell and bind to DNA. Obtained results were agreed with that achieved by Krajewska (Krajewska, Wydro, & Kyziol, 2013; Krajewska, Kyziol, & Wydro, 2013). Krajewska concluded that Hydrophobic character of chitosan has a role on disturbance of

Table 1
Enzymatic and non enzymatic degradation of chitosan, *O*-amine functionalized chitosan and the *N*-cinnamyl substituted *O*-amine functionalized chitosan.

	Nonenzymatic degradation (Optical Density)	Enzymatic degradation (Optical Density)
Chitosan	0.061 ± 0.003	0.357 ± 0.091
O-amine functionalized chitosan	0.042 ± 0.006	0.289 ± 0.087
The *N*-cinnamyl substituted *O*-amine functionalized chitosan	0.067 ± 0.004	0.251 ± 0.099

Table 2
Cytotoxicity studies of chitosan, *O*-amine functionalized chitosan and the *N*-cinnamyl substituted *O*-amine functionalized chitosan.

Material (mg)	Viable cells in the presence of chitosan (%)	Viable cells in the presence of *O*-amine functionalized chitosan (%)	Viable cells in the presence of the *N*-cinnamyl substituted *O*-amine functionalized chitosan (%)
25	97.4 ± 0.8	96.1 ± 0.5	96.2 ± 0.8
50	96.7 ± 0.5	94.2 ± 1.2	93.5 ± 0.8
100	95.1 ± 0.6	93.6 ± 1.3	92.4 ± 1.2
150	93.8 ± 0.7	92.1 ± 1.3	91.4 ± 1.3
200	90.4 ± 0.8	89.4 ± 1.4	88.1 ± 1.5

microorganisms cell wall membranes. This effect was maximized by raise hydrophobic character via modification. Therefore, the *N*-cinnamyl substituted *O*-amine functionalized chitosan can inhibit the bacterial propagation using the two proposed mechanisms, but the most acceptable is the first mechanism because of a high precipitation of the *N*-cinnamyl substituted *O*-amine functionalized chitosan as mentioned previously. It should also be noted that the antibacterial activity of these materials may least in part consist of disturbing cell membrane structures (Krajewska et al., 2013). For more details on the influence of pH and molecular weight on Chitosan interactions with membrane lipids the reader is referred to (Krajewska et al., 2011).

3.7. Biodegradability

Biodegradability of chitosan, *O*-amine functionalized chitosan and the *N*-cinnamyl substituted *O*-amine functionalized chitosan was assessed by determining the concentration of reducing sugar in the solution in the absence and presence of lysozyme as shown in Table 1. It is clear that in human serum *N*-acetylated chitosan is mainly depolymerized enzymatically by lysozyme, and not by other enzymes or other depolymerization mechanisms (Smidsrod, Varum, Myhr, & Hjerde, 1997). The enzyme degrades the polysaccharide *via* hydrolyzing the glycosidic bonds in the chemical structure. Lysozyme holds a hexameric binding site (Pangburn, Trescony, & Heller, 1982), and hexasaccharide sequences containing 3–4 or more acetylated units contribute mainly to the initial degradation rate of *N*-acetylated chitosan (Smidsrod et al., 1997). A general decrease in the degradation rate was observed by amination, then by Schiff base formation of chitosan. The appearance of additional bulk functional groups along the polymer backbone led to the formation of enzyme receptors.

3.8. *Cytotoxicity studies* in vitro

As shown in Table 2, the results of cytotoxicity of chitosan, *O*-amine functionalized chitosan and the *N*-cinnamyl substituted *O*-amine functionalized chitosan demonstrate slight differences between samples compared to the control cells. Previous papers proved that cytotoxicity of chitosan is affected by free amine group content, i.e. by the degree of deacetylation (Mohy Eldin, Soliman, Hashem, & Tamer, 2012). Results reveal that the highest amount tested (200 mg) of chitosan, *O*-amine functionalized chitosan and the *N*-cinnamyl substituted *O*-amine functionalized chitosan recorded 90.4%, 89.4%, and 88.1% of cell viability, respectively.

3.9. Rotational viscometry

Results in Fig. 6, black curves show a decrease in dynamic viscosity (η) of the HA solution (prepared in 0.15 M NaCl) exposed to oxidative degradation by the Weissberger biogenic oxidative system (WBOS) Valachova et al., (2016). According to WBOS, H_2O_2 molecules are generated as a result of the interaction of ascorbic acid with Cu(II) ions under aerobic conditions (Fisher & Naughton, 2005). Then, hydrogen peroxide was decomposed by the action of the intermediate Cu(I)--complex, thereby OH radicals are rapidly produced, which results in damaging of HA macromolecules.

Addition of acetic acid (0.5%) resulted in a faster degradation of HA. The decrease in η of the HA solution was 5.44 within 5 h (left panel, red curve). Chitosan and its derivatives added before HA degradation begins (a phase where OH radical is the dominant free radical species) decreased the rate of HA degradation (green, blue, and cyan curves) compared to the reference (black curve), which is due to the functional hydroxyl and amine groups (Muzzarelli, Muzzarelli, & Terbojerich, 1997; Park, Je, & Kim, 2004; Sousa, Guebitz, & Kokol, 2009; Xie, Xu, & Liu, 2001; Xue, Yu, Hirata, Terao, & Lin, 1998).

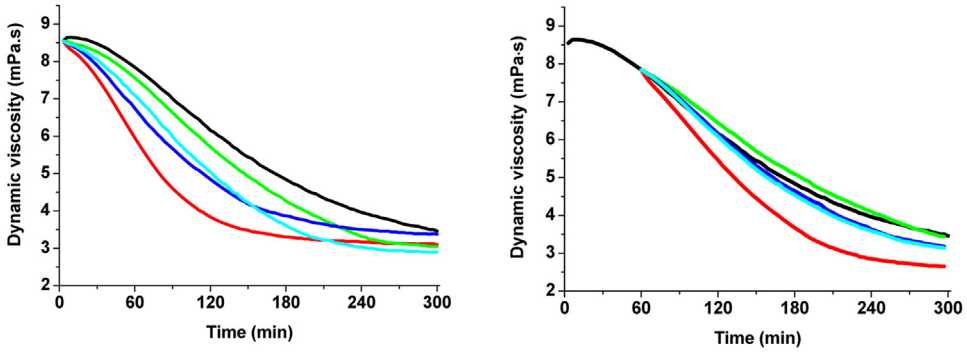

Fig. 6. HA degradation induced by WBOS (black curve). Effect of 0.5% acetic acid (red curves), and chitosan (green curve), *O*-amine functionalized chitosan (blue curve) and the *N*-cinnamyl substituted *O*-amine functionalized chitosan (cyan curve) when added to the reaction system before HA degradation begins (left panel) and 1 h later (right panel). (For interpretation of the references to colour in this figure legend, the reader is referred to the web version of this article.)

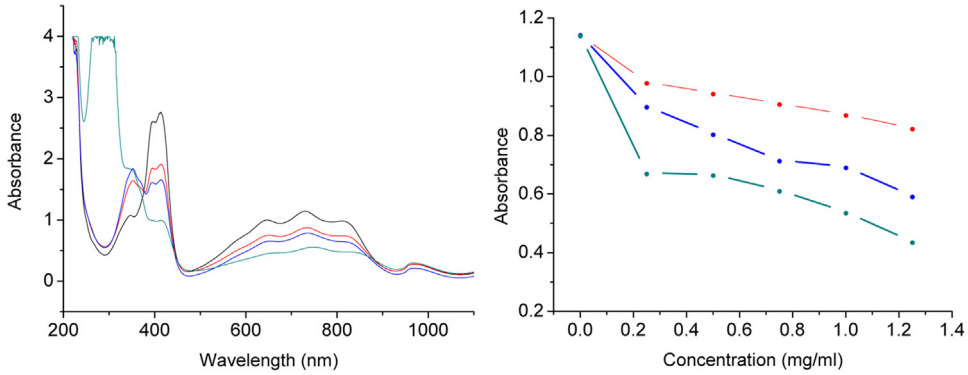

Fig. 7. Effect of chitosan (red), *O*-amine functionalized chitosan (blue) and the *N*-cinnamyl substituted *O*-amine functionalized chitosan (green) at concentration 1 mg/ml on reducing ABTS$^{\bullet+}$ cation (black) radical measured 10 min after the reaction onset (left panel). Effect of chitosan (red), *O*-amine functionalized chitosan (blue) and the *N*-cinnamyl substituted *O*-amine functionalized chitosan (green) at concentrations: 0, 0.25, 0.5, 0.75, 1.0 and 1.25 mg/ml on reducing ABTS$^{\bullet+}$ cation radical measured 10 min after the reaction onset (right panel). (For interpretation of the references to colour in this figure legend, the reader is referred to the web version of this article.)

Results in Fig. 6, right panel show the effect of the samples on the degradation of HA added one hour later, when hydroxyl radicals are supposed to be already consumed and radicals of alkoxy- and peroxy-types are dominant (Hrabarova, Valachova, Juranek, & Soltes, 2012; Valachova et al., 2011). All three tested derivatives partly reduced the degradative effects of the used solvent i.e. 0.5% acetic acid, however no one derivative was protective against HA degradation in the propagation phase of its decay by radicals of alkoxy- and peroxy-types Valachova et al., (2015).

3.10. ABTS assay

Fig. 7 (left panel) shows the decolorization of ABTS$^{\bullet+}$ by adding chitosan, *O*-amine functionalized chitosan and the *N*-cinnamyl substituted *O*-amine functionalized chitosan. The color of ABTS$^{\bullet+}$ was reduced by 23.4, 31.2 and 52.4% under influence of chitosan, *O*-amine functionalized chitosan and the *N*-cinnamyl substituted *O*-amine functionalized chitosan, respectively. The increase in decolorization of ABTS$^{\bullet+}$ from chitosan, *O*-amine functionalized chitosan to the *N*-cinnamyl substituted *O*-amine functionalized chitosan may be related to increasing the ability of chitosan derivatives to scavenge ABTS$^{\bullet+}$. Presence of cinnamyl nucleus along the polymer backbone promotes its ability to donate the electron. ABTS$^{\bullet+}$ exhibits a bluish-green color with maximum absorbance values at 645, 734, and 815 nm, this color rapidly disappears through electron from antioxidants (Re et al., 1999; Valachova et al., 2015; Hrabarova, Valachova, Rapta, & Soltes, 2010).

Figs. 7 (right panel) shows a dramatic concentration-dependent increase in decolorization effect of the tested polymer. At higher concentrations higher free radical scavenging capacities were observed. The electron-donating activity of the *N*-cinnamyl substituted *O*-amine functionalized chitosan is significantly higher than that of either chitosan itself or *O*-amine functionalized chitosan.

4. Conclusion

In this study, the *N*-cinnamyl substituted *O*-amine functionalized chitosan was prepared and characterized. Characteristic results show marked changes in its properties. It can be summarized as follows:

- The thermal stability of *O*-amine functionalized chitosan was enhanced with the incorporation of cinnamaldehyde.
- SEM analysis revealed that the prepared the *N*-cinnamyl substituted *O*-amine functionalized chitosan exhibited increased surface area due to roughness and porosity of the surface compared to *O*-amine functionalized chitosan or chitosan.
- The antibacterial evaluation demonstrates that this new Schiff base generated from *O*-amine functionalized chitosan exhibited better antibacterial activity than chitosan and *O*-amine functionalized chitosan.
- Antioxidant evaluation showing that the N-cinnamyl substituted O-amine functionalized chitosan has a lower tendency to scavenge OH radicals. On the other hand, it is a donor of electrons, which was demonstrated by the ABTS assay.

Acknowledgement

Work was supported by the grant VEGA2/0065/15.

Appendix A. Supplementary data

Supplementary data associated with this article can be found, in the online version, at http://dx.doi.org/10.1016/j.carbpol.2017.04.027.

References

Albadarin, A. B., Collins, M. N., Khraisheh, M., Walker, G., & Mangwandi, C. (2017). Activated lignin-chitosan extruded blends for efficient adsorption of methylene blue. *Chemical Engineering Journal, 307*, 264–272.
Anselmo, A. N., & Cobb, M. H. (2004). Protein kinase function and glutathionylation. *Biochemistry Journal, 381*, e1–e2.
Badawy, M. E. I., & Rabea, E. I. (2011). A biopolymer chitosan and its derivatives as promising antimicrobial agents against plant pathogens and their applications in crop protection. *International Journal of Carbohydrate Chemistry*, 1–29.
Baek, D., Jin, Y., Jeong, J. C., Lee, H. J., Moon, H., Lee, J., et al. (2008). Suppression of reactive oxygen species by glyceraldehyde-3-phosphate dehydrogenase. *Phytochemistry, 69*, 333–338.
Baldrick, P. (2010). The safety of chitosan as a pharmaceutical excipient. *Regulatory Toxicology and Pharmacology, 56*(3), 290–299.
Collins, M. N., & Birkinshaw, C. (2013a). Hyaluronic acid based scaffolds for tissue engineering – A review. *Carbohydrate Polymers, 92*, 1262–1279.
Collins, M. N., & Birkinshaw, C. (2013b). Hyaluronic acid solutions – A processing method for chemical modification. *Journal of Applied Polymer Science, 130*, 145–152.
Dodane, V., & Vilivalam, V. D. (1998). Pharmaceutical applications of chitosan. *Pharmaceutical Science & Technology Today, 1*, 246–253.
Dutta, J., Tripathi, S., & Dutta, P. K. (2011). Progress in microbial activities of chitin, chitosan and its oligosaccharides: A systematic study needs for food applications. *Food Science and Technology International, 18*, 3–34.
El-Sayed, E. M., Tamer, T. M., Omer, A. M., & Mohy Eldin, M. S. (2016). Development of novel chitosan schiff base derivatives for cationic dye removal: Methyl orange model. *Desalination and Water Treatment*, 1–14.
Fisher, A. E. O., & Naughton, D. P. (2005). Therapeutic chelators for the twenty first century: New treatments for iron and copper mediated inflammatory and neurological disorders. *Current Drug Delivery, 2*(3), 261–268.
Friedman, M., & Juneja, V. K. (2010). Review of antimicrobial and antioxidative activities of chitosans in food. *Journal of Food Protection, 73*, 1737–1761.

Gavalyan, V. B. (2016). Synthesis and characterization of new chitosan-based Schiff base compounds. *Carbohydrate Polymers, 145*, 37–47.
Hassan, M. A., Amara, A. A., Abuelhamd, A. T., & Haroun, B. M. (2010). Leucocytes show improvement growth on PHA polymer surface. *Pakistan Journal of Pharmaceutical Science, 23*, 332–336.
Hrabarova, E., Valachova, K., Rapta, P., & Soltes, L. (2010). An alternative standard for trolox-equivalent antioxidant-capacity estimation based on thiol antioxidants. Comparative 2, 2'-azinobis[3-ethylbenzothiazoline-6-sulfonic acid] decolorization and rotational viscometry study regarding hyaluronan degradation. *Chemistry & Biodiversity, 7*(9), 2191–2200.
Hrabarova, E., Valachova, K., Juranek, I., & Soltes, L. (2012). Free-radical degradation of high-molar-mass hyaluronan induced by ascorbate plus cupric ions: Evaluation of antioxidative effect of cysteine-derived compounds. *Chemistry & Biodiversity, 9*, 309–317.
Jeon, Y. J., Shahidi, F., & Kim, S. K. (2000). Preparation of chitin and chitosan oligomers and thir application in physiological functional foods. *Food Reviews International, 16*, 159–176.
Kean, T., & Thanou, M. (2010). Biodegradation, biodistribution and toxicity of chitosan. *Advanced Drug Delivery Reviews, 62*, 3–11.
Kenawy, E., Abdel-Hay, F. I., Mohy Eldin, M. S., Tamer, T. M., & Ibrahim, E. M. A. (2015). Novel aminated chitosan-aromatic aldehydes schiff bases: Synthesis, characterization, and bio-evaluation. *International Journal of Advanced Research, 3*, 563–572.
Kim, S. K., & Rajapakse, N. (2005). Enzymatic production and biological activities of chitosan oligosaccharides (COS): A review. *Carbohydrate Polymers, 62*, 357–368.
Kittur, F. S., Harish Prashanth, K. V., Udaya Sankar, K., & Tharanathan, R. N. (2002). Characterization of chitin: Chitosan and their carboxymethyl derivatives by. *Carbohydrate Polymers, 49*, 185–193.
Kong, M., Chen, X. G., Xing, K., & Park, H. J. (2010). Antimicrobial properties of chitosan and mode of action: A state of the art review. *International Journal of Food Microbiology, 144*, 51–63.
Krajewska, B., Wydro, P., & Janczyk, A. (2011). Probing the modes of antibacterial activity of chitosan Effects of pH and molecular weight on chitosan interactions with membrane lipids in Langmuir films. *Biomacromolecules, 12*, 4144–4152.
Krajewska, B., Kyziol, A., & Wydro, P. (2013). Chitosan as a subphase disturbant of membrane lipid monolayers: The effect of temperature at varying pH: II. DPPC and cholesterol. *Colloid. Surfaces. A, 434*, 359–364.
Krajewska, B., Wydro, P., & Kyziol, A. (2013). Chitosan as a subphase disturbant of membrane lipid monolayers. The effect of temperature at varying pH: I. DPPG. *Colloids and Surfaces a-Physicochemical and Engineering Aspects, 434*, 349–358.
Kumar, M. N., Muzzarelli, R. A., Muzzarelli, C., Sashiwa, H., & Domb, A. J. (2004). Chitosan chemistry and pharmaceutical perspectives. *Chemical Reviews, 104*, 6017–6084.
Kutyrev, A. A. (1991). Nucleophilic reactions of quinones. *Tetrahedron, 47*(38), 8043–8065.
Miller, G. L. (1959). Use of dinitrosalicylic acid reagent for determination of reducing sugar. *Analytical Chemistry, 31*, 426–428.
Mohy Eldin, M. S., Soliman, E. A., Hashem, A. I., & Tamer, T. M. (2008). Antibacterial activity of chitosan chemically modified with New Technique. *Trends in Biomaterials and Artificial Organs, 22*, 121–133.
Mohy Eldin, M. S., Soliman, E. A., Hashem, A. I., & Tamer, T. M. (2012). Antimicrobial activity of novel aminated chitosan derivatives for biomedical applications. *Advances in Polymer Technology, 31*, 414–428.
Mohy Eldin, M. S., Soliman, E. A., Hashem, A. I., Tamer, T. M., & Sabet, M. M. (2013). . *Antifungal Activity of aminated chitosan against three different fungi species* (Vol. 1) Key Engineering Materials-Current State-of-the-Art on Novel Materials [Chapter 26, ISBN: 9781926895734]
Mohy Eldin, M. S., Hashem, A. I., Omer, A. M., & Tamer, T. M. (2015a). Preparation: Characterization and antimicrobial evaluation of novel cinnamyl chitosan schiff base. *International Journal of Advanced Research, 3*, 741–755.
Mohy Eldin, M. S., Hashem, A. I., Omer, A. M., & Tamer, T. M. (2015b). Wound dressing membranes based on chitosan: Preparation, characterization and biomedical evaluation. *International Journal of Advanced Research, 3*(8), 908–922.
Moreno-Vásquez, M. J., Valenzuela-Buitimea, E. L., Plascencia-Jatomea, M., Encinas-Encinas, J. C., Rodríguez-Félix, F., Sánchez-Valdes, S., et al. (2017). Functionalization of chitosan by a free radical reaction: Characterization, antioxidant and antibacterial potential. *Carbohydrate Polymers, 155*, 117–127.
Mosmann, T. (1983). Rapid colorimetric assay for cellular growth and survival: Application to proliferation and cytotoxicity assays. *Journal of Immunological Methods, 65*, 55–63.
Muzzarelli, R. A. A., Muzzarelli, C. M., & Terbojerich, M. (1997). Chitin chemistry: Upgrading a renewable source. *Carbohydrate European, 19*, 10–17.
Pangburn, S. H., Trescony, P. V., & Heller, J. (1982). Lysozyme degradation of partially deacetylated chitin: Its films and hydrogels. *Journal of Biomaterials, 3*, 105–108.
Park, P. J., Je, J. Y., & Kim, S. W. (2004). Free radical scavenging activities of different deacetylated chitosans using ESR spectrometer. *Carbohydrate Polymers, 55*, 17–22.
Pawlak, A., & Mucha, M. (2003). Thermogravimetric and FTIR studies of chitosan blends. *Thermochimica Acta, 396*, 153–166.
Raafat, D., & Sahl, H. G. (2009). Chitosan and its antimicrobial potential – A critical literature survey. *Microbial Biotechnology, 2*, 186–201.
Rabea, E. I., Badawy, M. E., Stevens, C. V., Smagghe, G., & Steurbaut, W. (2003). Chitosan as an antimicrobial agent: Applications and mode of action. *Biomacromolecules, 4*, 1457–1465.
Ramnani, S. P., & Sabharwal, S. (2006). Adsorption behavior of Cr (VI) onto radiation crosslinked chitosan and its possible application for the treatment of waste water containing Cr (VI). *Reactive and Functional Polymers, 66*, 902–909.
Rapta, P., Valachova, K., Gemeiner, P., & Soltes, L. (2009). High-molar-mass hyaluronan behavior during testing its radical scavenging capacity in organic and aqueous media: Effects of the presence of manganese(II) ions. *Chemistry & Biodiversity, 6*, 162–169.
Re, R., Pellegrini, N., Proteggente, A., Pannala, A., Yang, M., & Rice-Evans, C. (1999). Antioxidant activity applying an improved ABTS radical cation decolorization assay. *Free Radical Biology & Medicine, 26*, 1231–1237.
Shahidi, F., Arachchi, J. K. V., & Jeon, Y. (1999). Food application of chitin and chitosan. *Trends in Food Science & Technology, 10*, 37–51.
Skyttä, E., & Mattila, S. T. (1991). A quantitative method for assessing bacteriocins and other food antimicrobials by automated turbidometry. *Journal of Microbiological Methods, 14*, 77–88.
Smidsrod, O., Varum, K. M., Myhr, M. M., & Hjerde, R. J. N. (1997). In vitro degradation rates of partially N-acetylated chitosans in human serum. *Carbohydrate Research, 299*, 99–101.
Soliman, E. A., El-Kousy, S. M., Abd-Elbary, H. M., & Abou-zeid, A. R. (2013). Low molecular weight chitosan-based schiff bases: Synthesis, characterization: and antibacterial activity. *American Journal of Food Technology, 8*, 17–30.
Soltes, L., Stankovska, M., Kogan, G., Gemeiner, P., & Stern, R. (2005). Contribution of oxidative-reductive reactions to high-molecular-weight hyaluronan catabolism. *Chemistry & Biodiversity, 2*, 1242–1246.
Soltes, L., Kogan, G., Stankovska, M., Mendichi, R., Rychly, J., Schiller, J., et al. (2007). Degradation of high-molar-mass hyaluronan and characterization of fragments. *Biomacromolecules, 8*(9), 2697–2705.
Sousa, F., Guebitz, G. M., & Kokol, V. (2009). Antimicrobial and antioxidant properties of chitosan enzymatically functionalized with flavonoids. *Process Biochemistry, 44*, 749–756.
Sreenivasan, K. (1996). Thermal stability studies of some chitosan – Metal ion complexes using differential scanning calorimetry. *Polymer Degradation and Stability, 52*, 85–87.
Stammati, A., Bonsi, P., Zucco, F., Moezelaar, R., Alakomi, H. L., & von Wright, A. (1999). Toxicity of selected plant volatiles in microbial and mammalian short-term assays. *Food Chem. Toxicol., 37*, 813–823.
Tamer, T. M., Valachova, K., & Soltes, L. (2014). Inhibition of free radical degradation in medical grade hyaluronic acid. In N. Maurice Collins (Ed.), *Hyaluronic acid for biomedical and pharmaceutical applications*. Smither Rapra Publishers.
Tamer, M. T., Omer, A. M., Hassan, M. A., Hassan, M. E., Sabet, M. M., & Mohy Eldin, M. S. (2015). Development of thermo-sensitive poly *N*-isopropyl acrylamide grafted chitosan derivatives. *Journal of Applied Pharmaceutical Science, 5*, 1–6.
Tamer, T. M., Valachova, K., Mohy Eldin, M. S., & Soltes, L. (2016). Free radical scavenger activity of cinnamyl chitosan schiff base. *Journal of Applied Pharmaceutical Science, 6*, 130–136.
Tamer, T. M., Valachova, K., Mohyeldin, M. S., & Soltes, L. (2016). Free radical scavenger activity of chitosan and its aminated derivative. *Journal of Applied Pharmaceutical Science, 6*, 195–201.
Valachova, K., Vargova, A., Rapta, P., Hrabarova, E., Drafi, F., Bauerova, K., et al. (2011). Aurothiomalate as preventive and chain-breaking antioxidant in radical degradation of high-molar-mass hyaluronan. *Chemistry Biodiversity, 8*(7), 1274–1283.
Valachova, K., Banasova, M., Topolska, D., Sasinkova, V., Juranek, I., Collins, M. N., et al. (2015). Influence of tiopronin: captopril and levamisole therapeutics on the oxidative degradation of hyaluronan. *Carbohydrate Polymers, 134*, 516–523.
Valachova, K., Topolska, D., Mendichi, R., Collins, M. N., Sasinkova, V., & Soltes, L. (2016). Hydrogen peroxide generation by the Weissberger biogenic oxidative system during hyaluronan degradation. *Carbohydrate Polymers, 148*, 189–193.
Vinsova, J., & Vavríková, E. (2011). Chitosan derivatives with antimicrobial, antitumor and antioxidant activities – A review. *Current Pharmaceutical Design, 17*, 3596–3607.
Waris, G., & Ahsan, H. (2006). Reactive oxygen species: role in the development of cancer and various chronic conditions. *Journal of Carcinogenesis, 5*, 1–8.
Xie, W., Xu, P., & Liu, Q. (2001). Antioxidant activity of a water-soluble chitosan derivates. *Bioorganic & Medicinal Chemistry Letters, 11*, 1699–1701.
Xiong, S. L., Li, A. L., Jin, Z. Y., & Chen, M. (2007). Effects of oral chondroitin sulfate on lipid and antioxidant metabolisms in rats fed a high-fat diet. *Journal of Food Biochemistry, 31*, 356–369.
Xue, C., Yu, G. T., Hirata, J., Terao, J., & Lin, H. (1998). Antioxidative activities of several marine polysacharides evaluated in a phosphatidylcholine-liposomal suspension and organic solvents. *Bioscience Biotechnology and Biochemistry, 62*, 206–209.
Zawadzki, J., & Kaczmarek, H. (2010). Thermal treatment of chitosan in various conditions. *Carbohydrate Polymers, 80*, 394–400.
dos Santos, J. E., Dockal, E. R., & Cavalheiro, T. G. (2005). Thermal behavior of Schiff bases from chitosan. *Journal of Thermal Analysis and Calorimetry, 79*, 243–248.